

We are IntechOpen, the world's leading publisher of Open Access books Built by scientists, for scientists

6,900

Open access books available

186,000

International authors and editors

200M

Downloads

Our authors are among the

154

Countries delivered to

TOP 1%

most cited scientists

12.2%

Contributors from top 500 universities



WEB OF SCIENCE™

Selection of our books indexed in the Book Citation Index
in Web of Science™ Core Collection (BKCI)

Interested in publishing with us?
Contact book.department@intechopen.com

Numbers displayed above are based on latest data collected.
For more information visit www.intechopen.com



Influence of Branching Patterns and Active Contractions of the Villous Tree on Fetal and Maternal Blood Circulations in the Human Placenta

Yoko Kato

Additional information is available at the end of the chapter

<http://dx.doi.org/10.5772/intechopen.79343>

Abstract

In the human placenta, fetal blood circulates in the blood vessels of the villous tree while maternal one circulates in the intervillous space, the surroundings of the villous tree. Previously, the computational model of the villous tree, whose stem villi actively contract because of the contractile cells, has been developed. The result of the computation indicated that the displacement caused by the contraction would be helpful for the fetal and maternal circulations and can be combined with the other measurements for blood circulations in the placenta. Hypoxia in the placenta is classified into the following categories: preplacental hypoxia, uteroplacental hypoxia, and postplacental hypoxia. The number and the form of the terminal villi are altered by hypoxia. Assuming that increase in the terminal villi causes a higher shear elastic modulus of the placenta, this villous tree model is useful to estimate the influence of hypoxia on the blood circulations. In this chapter, how these three types of hypoxia influence the blood circulation in the placenta by the aforementioned computational model are discussed. While preplacental hypoxia and uteroplacental hypoxia would cause similar displacement in large regions, postplacental hypoxia would do vice versa. All the types might make the fetal and maternal blood circulations difficult.

Keywords: placenta, hypoxia, villous tree, terminal villi, contraction, blood circulation

1. Introduction

In the human placenta, the blood vessels in the villous tree lead to the umbilical artery and vein, while the intervillous space, the surroundings of the villous tree, is linked to the uterine artery

and vein. The fetal and maternal blood circulates separately so that the substances and gases are exchanged through the surface of the villous tree, without mixing these two types of blood [1]. The influence of the blood circulations on the exchange of the substances has been investigated [2, 3]. Also, the fetal and maternal blood circulations in the placenta have been evaluated by ultrasound Doppler and MRI so that the influences of these circulations on fetal growth have been indicated [4–9]. However, the direction of the blood flow in the placenta has been hardly determined yet.

The villous tree is classified into the following villous types: stem villi, intermediate villi, terminal villi, and mesenchymal villi [1, 10]. At term, the villous tree is mainly composed of stem villi, mature intermediate villi, and terminal villi [1, 11, 12]. The stem villi, the main support of the villous tree, are connected to the mature intermediate villi, which is accompanied by the terminal villi. In the stem villi, arteries, veins, arterioles, venules, and capillaries are observed [1, 11]. The mature intermediate villi have arteriole, postcapillary venules, and capillaries, part of which are linked to the capillary loop in the terminal villi [1, 12]. The artery and vein in the stem villi are surrounded by contractile cells, which are axially aligned [13–20]. Also, the contraction of the stem villi has been observed [14, 21–23].

Since the contraction of the stem villi would contribute to the fetal and maternal blood circulations in the placenta, the computational model of the villous tree, which actively contracts, has been developed [24]. In this model, the contraction of the stem villi causes the displacement of the surroundings: the displacement propagates from the surface of the stem villi. The result of the computation based on this model indicated that the magnitude of the displacement was almost kept in the placenta, and the direction was helpful for the fetal and maternal circulations although several positions were vulnerable to the mechanical properties of the placenta [24]. In addition, the comparison between the displacement pattern estimated by this model and flow velocity measured by the aforementioned methods will provide the direction of the blood flow in the placenta [24]. However, how the parameters in this computation, including the shear elastic modulus of the placenta and the maximum distance for the propagation, influence the displacement has not been investigated yet.

Hypoxia is classified into the following groups: preplacental hypoxia, less oxygen content in the maternal blood; uteroplacental hypoxia, normal oxygen content in the maternal blood but less content in the uteroplacental tissues; postplacental hypoxia, normal oxygen content in the maternal blood but less content in the fetus because of the problem in the fetoplacental perfusion [1, 25, 26]. In preplacental hypoxia and uteroplacental hypoxia, capillaries are highly branched and the terminal villi are clustered so that the terminal villi are predominantly observed [1, 25, 26]. The terminal villi in postplacental hypoxia are filiform and scarcely observed [1, 25, 26]. The villous tree model, which changes its shape based on the oxygen content, has also developed [27]. Assuming that an increase in the terminal villi is corresponding to the higher shear elastic modulus of the placenta and longer propagation distance of the stem villi contraction, the stem villi model [24] is useful to estimate the influence of hypoxia on the blood circulation in the placenta. However, such an analysis has not been done yet.

In this chapter, how three kinds of hypoxia influence the blood circulations in the placenta was evaluated. The computational model of the stem villi has been developed and used to estimate the distribution of the displacement in the placenta previously [24]. The distribution of the displacement was analyzed not for hypoxia, but for general characteristics of the

displacement so that the influences of the parameters such as the shear elastic modulus and distance for the propagation on the displacement have barely investigated. After introducing the model of the villous tree, the analyses for the influences of these parameters on the displacement and characteristics of the displacement in hypoxia were indicated.

2. Computational models

2.1. Villous tree model

The computational model and parameters have been reported previously [24]. **Figure 1** shows the computational model, where the chorionic and basal plates are the boundaries for the fetal and maternal sites, respectively. Truncus chorii, rami chorii, and ramuli chorii are parts of the stem villi. The position in the model is indicated by the Cartesian coordinate: the z axis, whose origin is placed on the chorionic plate, perpendicular to the chorionic and basal plates. That is, the z coordinate is corresponding to the distance from the chorionic plate. The surroundings of the stem villi are composed of the intervillous space, where the maternal blood circulates, and all the villi except the stem villi. The size and branching patterns based on the histological reports [1, 10] were as follows: diameter, 3–0.3 mm; branching pattern, no bifurcation in the truncus chorii, equally dichotomous as well as symmetric in the rami chorii, and unequally dichotomous as well as asymmetric in the ramuli chorii.

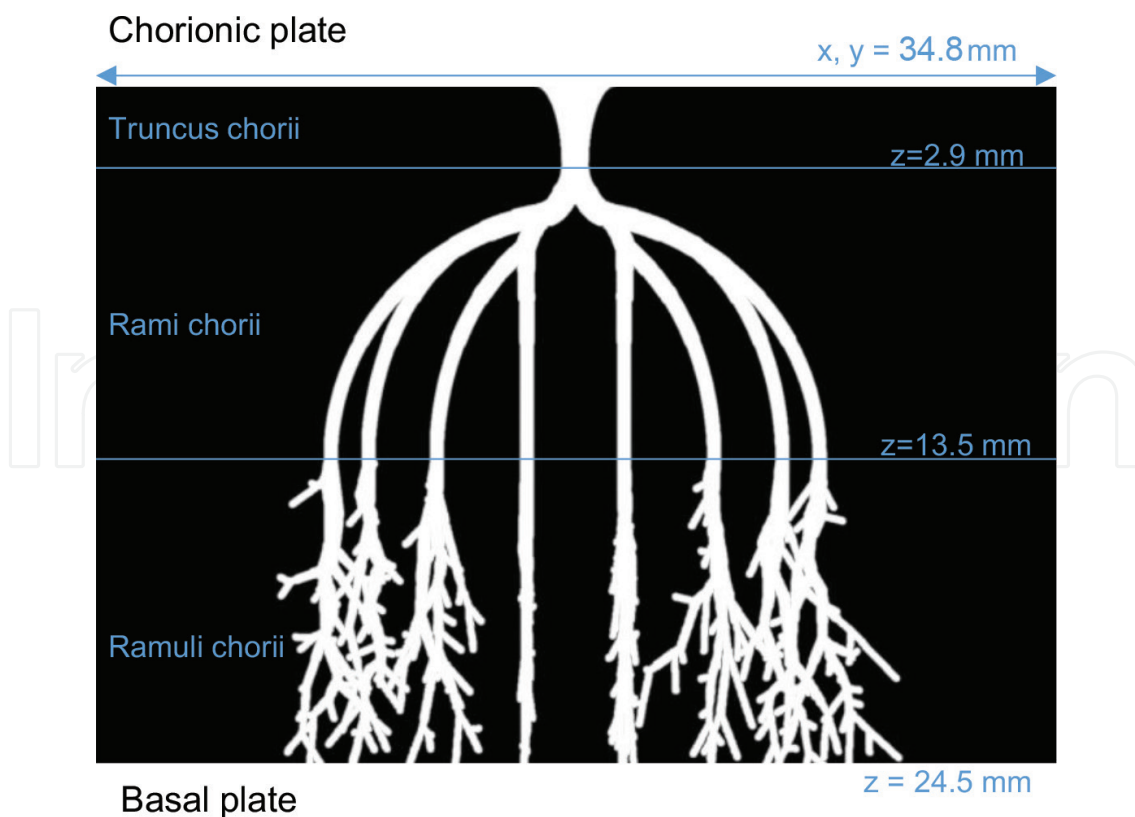


Figure 1. Side view of the villous tree model. White region, stem villi; black region, other types of villi and intervillous space; size (x, y, z), $1200 \times 1200 \times 847$ pixels (1 pixel = $29 \mu\text{m}$) (source: modified from Figure 1 in Kato et al. [24]).

The displacement, u , is described by the following equation:

$$u = \xi_0 \cos kr \quad (1)$$

where ξ_0 is the amplitude (0.1 μm), k is the wavenumber and r is the distance from the surface of the stem villi. The maximum distance for the propagation, s , was 1.45, 2.9, or 4.35 mm. Also, the shear elastic modulus, μ , is described as follows:

$$\mu = \rho \lambda^2 \nu^2 \quad (2)$$

where ρ is the density ($1.0 \times 10^3 \text{ kg/m}^3$), λ is the wavelength (0.29, 0.58, or 1.45 mm), and ν is the frequency (1 Hz). Hence, the shear elastic modulus of the placenta was $8.41 \times 10^{-5} \text{ Pa}$, $3.36 \times 10^{-4} \text{ Pa}$, or $2.10 \times 10^{-3} \text{ Pa}$. The displacement caused by the contraction was indicated by the polar coordinate: magnitude, ϕ (0 to 180°) and θ (-180 to 180°).

2.2. Hypoxia model

The villous tree in preplacental hypoxia and uteroplacental hypoxia has plenty of terminal villi while that in postplacental hypoxia has few filiform ones [1, 25, 26]. It was assumed that an increase in the number of the terminal villi makes the shear elastic modulus of the placenta higher and the maximum distance for the propagation of the displacement longer. Because the model, whose shear elastic modulus was $3.36 \times 10^{-4} \text{ Pa}$, was the control model, the shear elastic moduli in the preplacental hypoxia and uteroplacental hypoxia model and the postplacental hypoxia model were 2.10×10^{-3} and $8.41 \times 10^{-5} \text{ Pa}$, respectively. Also, the maximum distances for the displacement propagation of the preplacental hypoxia and uteroplacental hypoxia model and the postplacental model were 4.35 and 1.45 mm, respectively, since that of the control model was 2.9 mm. Because the shear elastic moduli and the maximum distance for the propagation had three types, respectively, nine different models were made. The models except the control model, the preplacental hypoxia and uteroplacental hypoxia model, and the postplacental model represent the conditions toward these types of hypoxia.

2.3. Contraction

Three types of hypoxia in the placenta alter the terminal villi but rarely the stem villi. How the hypoxia influences the contractile cells in the stem villi has been barely investigated. The previous report has indicated that fetal growth restriction enhances α -smooth muscle actin of the stem villi [28]. Hence, the amplitude, ξ_0 , in Eq. (1) could be maintained in all the models but also be changed as 0.4 μm for $8.41 \times 10^{-5} \text{ Pa}$, 0.016 μm for $2.10 \times 10^{-3} \text{ Pa}$ because of the change in the elastic moduli.

2.4. Characteristic positions

In order to evaluate the influence of the terminal villi on the displacement distribution in the placenta, the mean and standard deviation of the magnitude, ϕ and θ in each z coordinate were used as the previous report indicated [24]. The middle positions of each part and several z coordinates which show the characteristic distributions of the magnitude, ϕ , and θ are used: z_{ν} , z_r , and $z_{\nu r}$ the middle positions of the truncus chorii, rami chorii, and ramuli chorii; $z_{sd/mean}$

the z coordinate at the peak of the standard deviation normalized by the mean in the displaced area; $z_{\phi 1}$ and $z_{\phi 2}$, the z coordinates at the lower and higher peaks of the standard deviation of ϕ , respectively; $z_{\phi'}$, the z coordinate at the lower peak of the mean from the rami chorii to the ramuli chorii. These positions have been used previously [24], but how the parameters influence the positions have not been investigated yet.

2.5. Statistical analysis

The coefficient of determination, R^2 , in the regression line, and the number of the samples, n , provide F-value, F , whose $df1$ and $df2$ were 1 and $n-2$, respectively:

$$F = n-2 \frac{R^2}{1-R^2} \quad (3)$$

The level of significance was 0.05.

3. Results

3.1. Displaced region

Figure 2 shows that the displaced volume normalized by the volume of the entire model except the stem villi region became larger as the maximum distance for the propagation, s , grew longer. However, the wavelength scarcely altered the size of the displaced region.

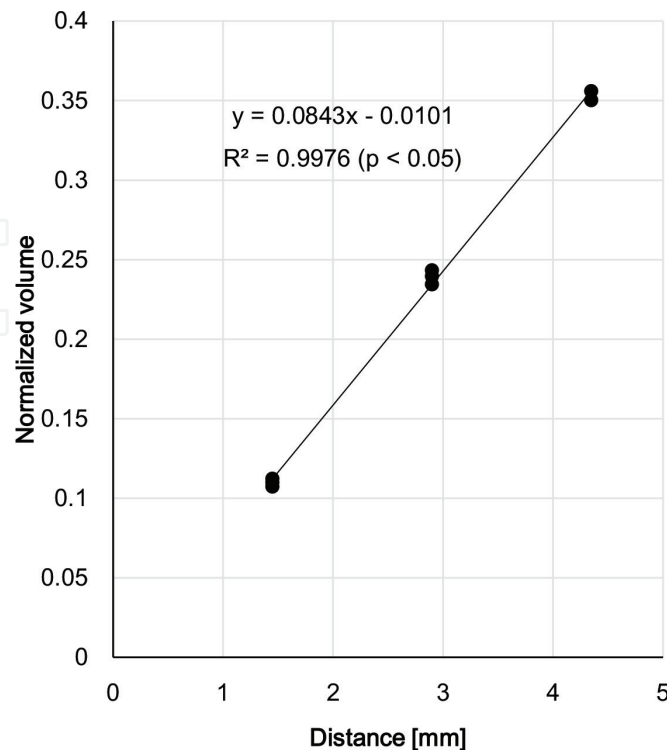


Figure 2. Displaced volume normalized by the volume of the model except the stem villi ($2.96 \times 10^4 \text{ mm}^3$).

These results indicate that the displaced area in the placenta under preplacental hypoxia and uteroplacental hypoxia would be larger than that under postplacental hypoxia.

Figure 3 shows the displaced area at the control model. Since the wavelength weakly influences the size of the displaced region, the mean of the displaced area at the same maximum distance for the propagation in each characteristic z coordinate was calculated. **Figure 4** shows the relationship between the displaced area normalized by that at the maximum distance for the propagation of the control model (2.9 mm) and the characteristic z coordinates. The maximum distance for the propagation almost equally altered the size of the displaced area at all the characteristic position except z_t and $z_{sd/mean}$ at both of the maximum distances. The influence of the maximum distance on the size of the displaced area at z_t and $z_{sd/mean}$ were much larger than that on the other positions. Considering that z_t and $z_{sd/mean}$ are close to the chorionic plate, all the types of hypoxia would strongly influence the blood circulations near the chorionic plate.

3.2. Characteristic positions

Figure 5 shows that the maximum distance for the propagation scarcely influenced the characteristic z positions. The influence of the wavelength was also little. Hence, the characteristic z positions would be kept in all the types of hypoxia.

3.3. Displacement: magnitude

Figures 6 and 7 show the mean of the displacement in each model when the amplitude ξ_0 was maintained. As the wavelength and maximum distance for the propagation grew

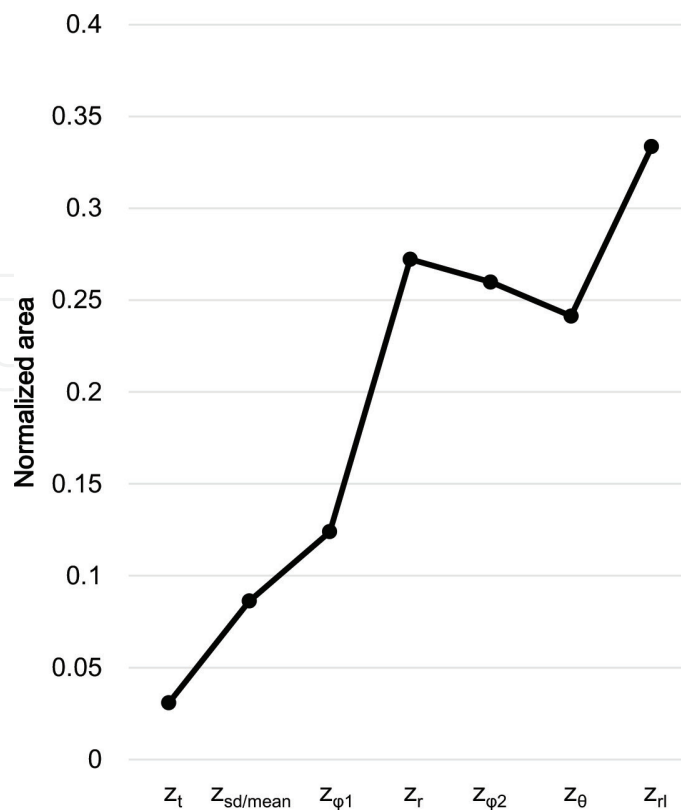


Figure 3. Displaced area normalized by the area of the model at each z coordinate. $\lambda = 0.58$ mm and $s = 2.9$ mm.

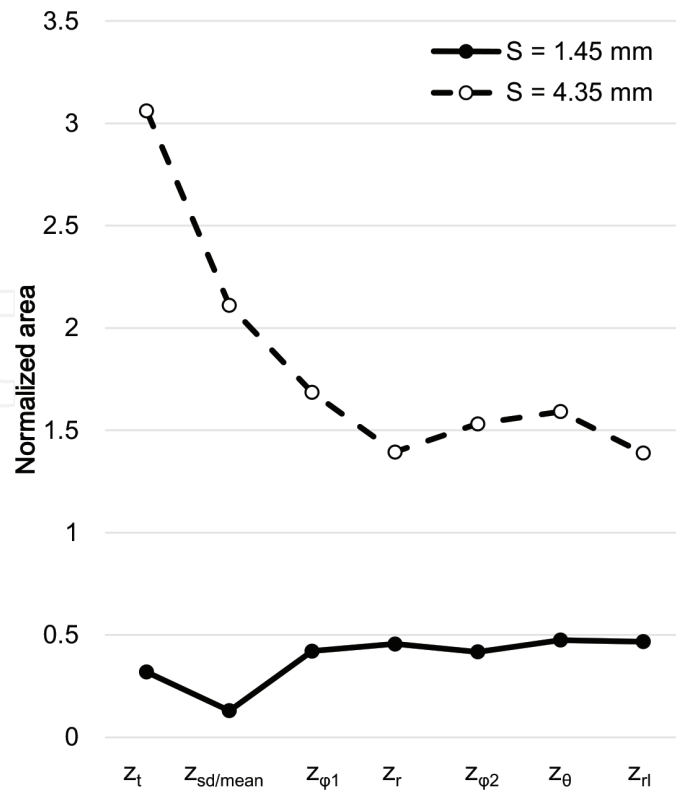


Figure 4. Displaced area normalized by that of the model for $s = 2.9$ mm at the characteristic z coordinates. The displaced area in each model ($s = 1.45, 2.9,$ and 4.35 mm) was averaged.

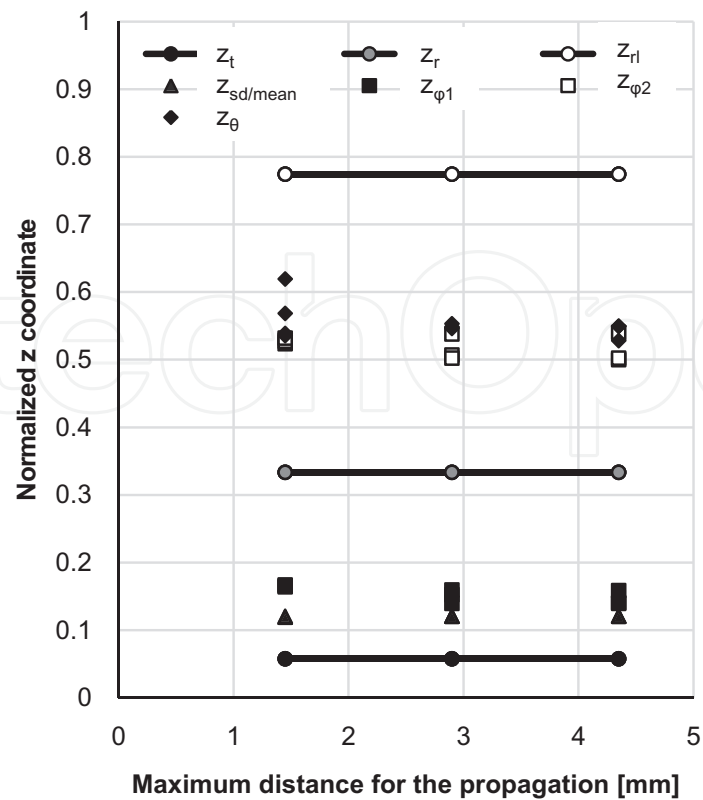


Figure 5. Distance from the characteristic positions to the chorionic plate normalized by that between the chorionic and basal plates.

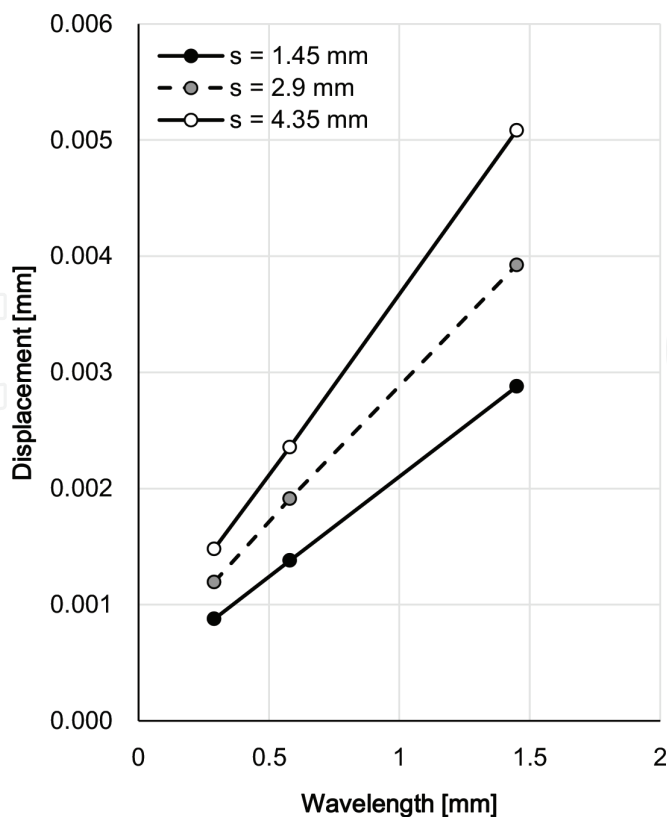


Figure 6. Influence of the wavelength on the mean of the displacement in each model.

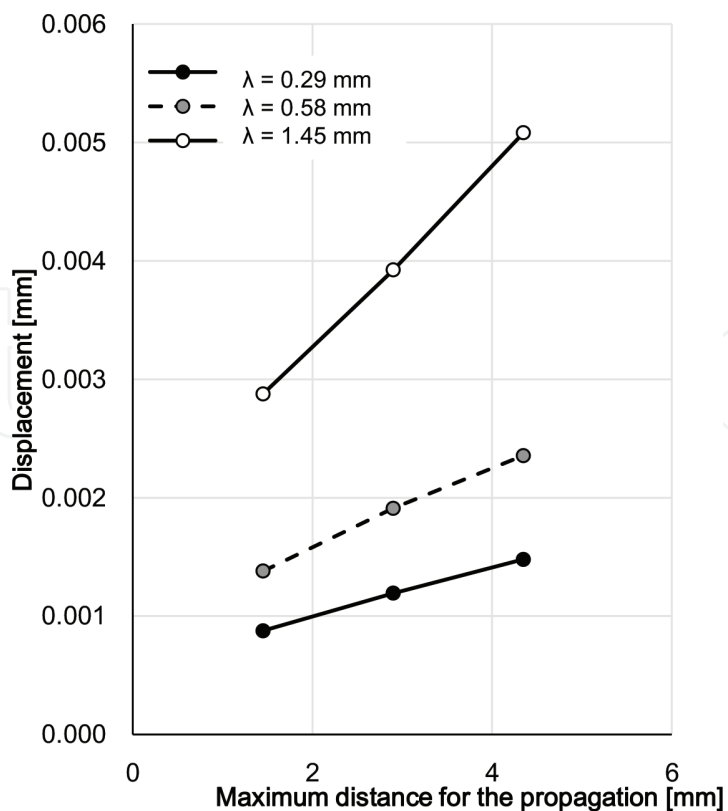


Figure 7. Influence of the maximum distance for the propagation on the mean of the displacement in each model.

longer, the displacement became larger. When ξ_0 became smaller as the shear elastic modulus of the placenta grew larger, the mean of the displacement was largely decreased by the longer wavelength as **Figure 8** shows. In **Figure 9**, the longer distance for the propagation induced the larger displacement as shown in **Figure 7**. However, the longer wavelength induced the larger displacement in **Figure 7** but vice versa in **Figure 9**. Considering that the preplacental hypoxia and uteroplacental hypoxia model, and the postplacental hypoxia model showed the smallest elastic moduli and maximum distance, and the largest ones, the mean of the displacement would be different from the control model as shown in **Figures 6–9**.

3.4. Displacement: direction (ϕ and θ)

While **Figure 10** shows that the influence of the wavelength on the range of the area fraction for $\phi = 45\text{--}135^\circ$ among those at the characteristic z coordinates was barely consistent, the longer maximum distance for the propagation reduced the range as shown in **Figure 11**. Hence, the longer maximum distance for the propagation would weaken the influence of the z coordinate on ϕ .

Both the wavelength and the maximum distance for the propagation influenced the standard deviation of the area fraction in each class interval of θ (SDin), but not consistently. SDin at z_r was decreased by the longer wavelength and maximum distance as shown in **Figure 12**. SDin at z_l indicated the same tendency, but those at z_t and z_0 did not.

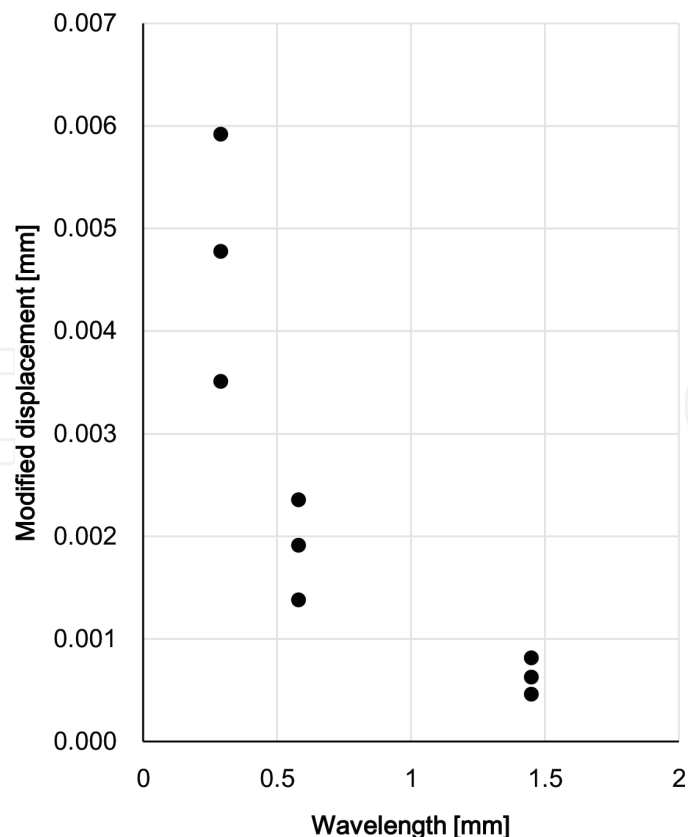


Figure 8. Influence of the wavelength on the mean of the modified displacement.

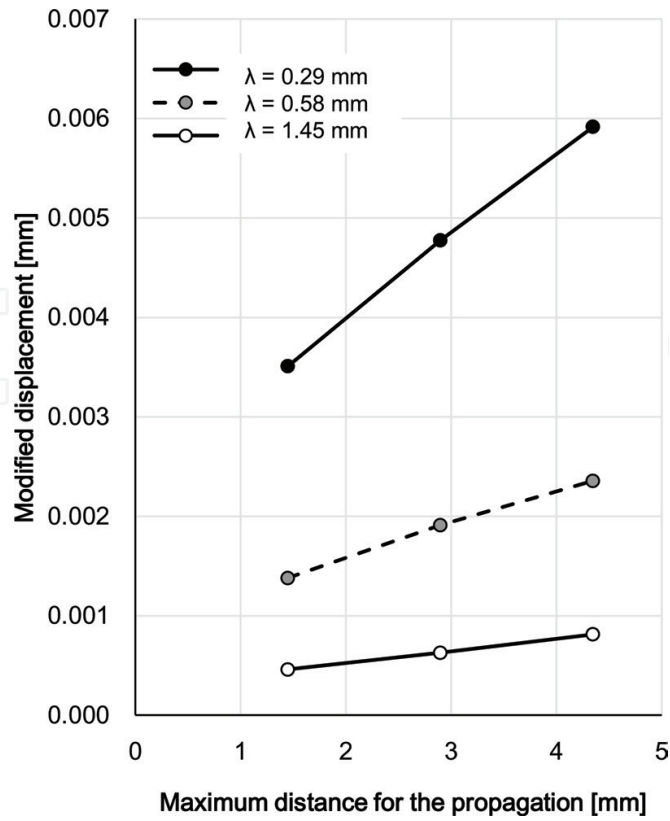


Figure 9. Influence of the maximum distance for the propagation on the mean of the modified displacement.

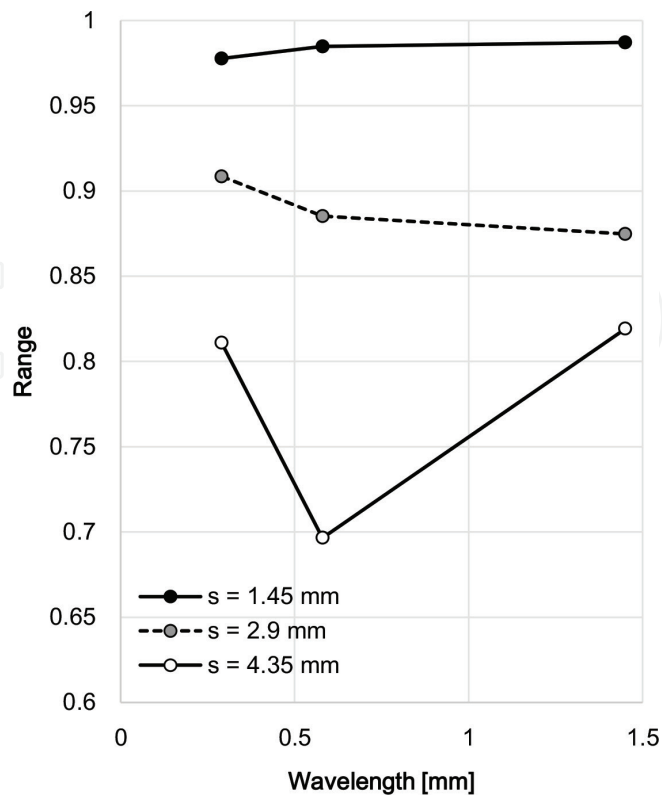


Figure 10. Influence of the wavelength on the range of the area fraction for the displaced area at $\phi = 45\text{--}135^\circ$.

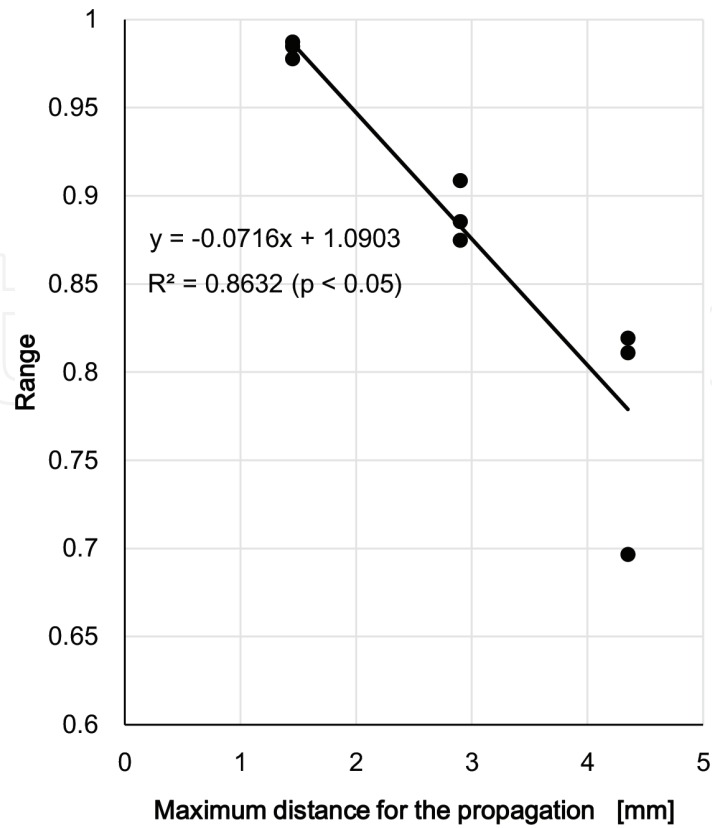


Figure 11. Influence of the Maximum distance for the propagation on the range of the area fraction for the displaced area at $\phi = 45\text{--}135^\circ$.

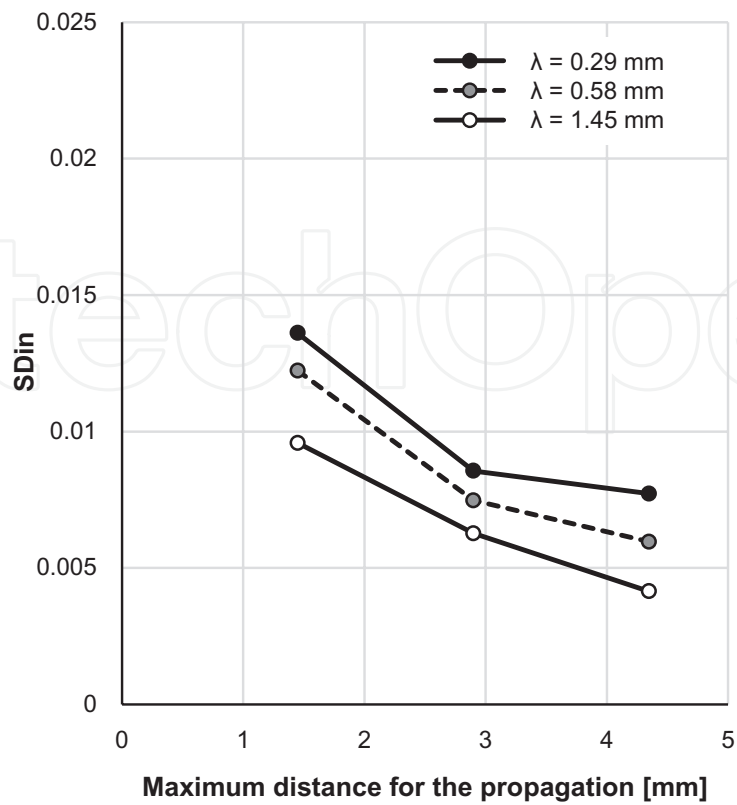


Figure 12. The standard deviation of the area fraction in each class interval of θ (SDin) at the rami chorii.

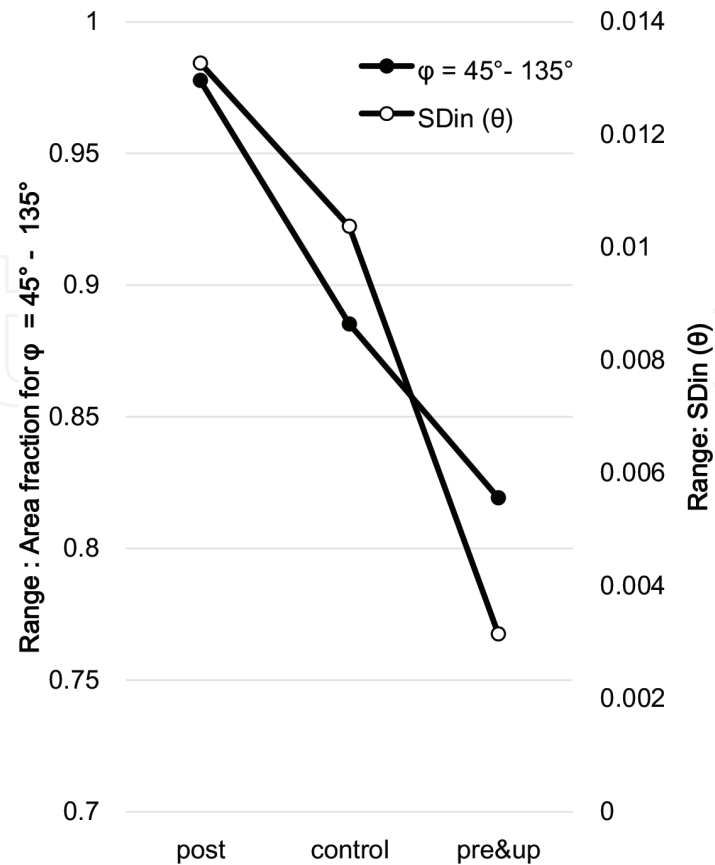


Figure 13. The range of the area fraction for $45\text{--}135^\circ$, and range of SDin (θ). Post, postplacental hypoxia; pre&up, preplacental hypoxia and uteroplacental hypoxia.

Figure 13 shows the ranges of the area fraction for $\phi = 45\text{--}135^\circ$ and SDin at the control model ($s = 2.9$ mm, $\mu = 3.36 \times 10^{-4}$ Pa), postplacental hypoxia model ($s = 1.45$ mm, $\mu = 8.41 \times 10^{-5}$ Pa), and preplacental hypoxia and uteroplacental hypoxia model ($s = 4.35$ mm, $\mu = 2.10 \times 10^{-3}$ Pa). In both ranges, the postplacental hypoxia model was the largest while the preplacental and uteroplacental hypoxia model was the smallest. The result described that the direction of the displacement in the postplacental hypoxia model was more varied than that in the preplacental hypoxia and uteroplacental hypoxia model.

4. Discussion

In this chapter, the displacement caused by the contraction of the stem villi in the three types of hypoxia in the placenta was evaluated. While the villous tree is rich in terminal villi at preplacental hypoxia and uteroplacental hypoxia, it has few terminal villi at postplacental hypoxia. Assuming that increase in the terminal villi in the placenta induces higher shear elastic moduli of the placenta, postplacental hypoxia would show lower shear elastic moduli while preplacental hypoxia and uteroplacental hypoxia would show higher ones. In the meantime, the computational model of the villous tree with active contractions has been developed

previously [24], and it has been shown that the magnitude and direction of the displacement would be helpful for the blood circulation in the placenta [24]. Because the general aspects of the displacement caused by the contraction were investigated in the previous study [24], the influence of each parameter on the displacement and how to modulate the parameter and model for representing the dysfunction of the placenta, including hypoxia, has been barely discussed. Based on the previous computation [24], the analysis for the preplacental hypoxia and uteroplacental hypoxia model and the postplacental hypoxia model was done.

The maximum propagation distance influenced the displaced region, especially near the chorionic plate. However, the characteristic z coordinates, was not influenced by the shear elastic modulus and the maximum propagation distance. When increase in the shear elastic modulus of the placenta reduced the displacement caused by the contraction of the stem villi, the placenta in preplacental hypoxia or uteroplacental hypoxia caused smaller displacement than that in postplacental hypoxia. Also, changes in the magnitude and direction of the displacement would occur at the characteristic positions, kept in all the models. The range of the area fraction for the displaced area at $\phi = 45\text{--}135^\circ$ got smaller as the maximum distance for the propagation became longer. The influence of the wavelength and the maximum distance for the propagation on the standard deviation of the area fraction in each class interval of θ (SDin) was dependent on the z coordinates. The SDin was more influenced by the z coordinates than the wavelength and the maximum distance so that SDin would be dependent on the shape of the stem villi. The ranges of the area fraction at $\phi = 45\text{--}135^\circ$ and SDin in the postplacental hypoxia model was larger than those in the preplacental hypoxia and uteroplacental hypoxia model. Postplacental hypoxia would cause more varied displacement pattern than preplacental hypoxia and uteroplacental hypoxia.

According to the aforementioned results, postplacental hypoxia would have the small region displaced with various directions, and preplacental hypoxia and uteroplacental hypoxia would have the large region displaced with similar directions. In the intervillous space, the maternal blood in postplacental hypoxia might hardly circulate around the villous tree because of the small displacement regions with various directions while that in preplacental hypoxia and uteroplacental hypoxia might experience difficulties in circulation because of the large region displaced with similar directions. In the terminal villi, the fetal blood in postplacental hypoxia might have difficulty in circulation because the small amount of the capillaries would be received the displacement with various directions while that preplacental hypoxia and uteroplacental hypoxia might flow in the capillaries with difficulties because the large amount of the fetal blood would receive the displacement with similar directions.

The villous tree model enables us to depict the displacement pattern in the placenta, which is linked to the mechanical environment. It is possible to apply the mechanical environment to the computation about the model of the terminal villi, which is composed of the capillaries [29]. In the meantime, telocytes in the placenta have been found [30–33]. The distribution of the telocytes should be considered because the placenta is an innervated organ. Moreover, a novel medical imaging method available for the placenta [34] is also developed. If the villous tree model and the aforementioned findings and methods are combined together, dysfunctions in the placenta can be estimated more precisely.

5. Conclusion

In this chapter, how hypoxia influences the displacement caused by the contraction of the stem villi was estimated. Preplacental hypoxia and uteroplacental hypoxia would cause similar displacement directions in large regions while postplacental hypoxia would cause small displaced regions with various directions. Both of them might cause difficulties for the fetal and maternal circulations in the placenta.

Conflict of interest

None.

Author details

Yoko Kato

Address all correspondence to: ykato@mail.tohoku-gakuin.ac.jp

Faculty of Engineering, Tohoku Gakuin University, Tagajo, Miyagi, Japan

References

- [1] Benirschke K, Burton GJ, Baergen RN. Pathology of the human placenta. 6th ed. Berlin Heidelberg: Springer-Verlag; 2012 . 941p. DOI: 10.1007/978-3-642-23941-0
- [2] Illsley NP, Hall S, Stacey TE. The modulation of glucose transfer across the human placenta by intervillous flow rates: An in vitro perfusion study. *Trophoblast Research*. 1987;**2**:535-544
- [3] Lofthouse EM, Perazzolo S, Brooks S, Crocker IP, Glazier JD, Johnstone ED, Panitchob N, Sibley CP, Widdows KL, Sengers BG, Lewis RM. Phenylalanine transfer across the isolated perfused human placenta: Experimental and modelling investigation. *American Journal of Physiology. Regulatory, Integrative and Comparative Physiology*. 2015; **310**(9):R828-R836. DOI: 10.1152/ajpregu.00405.2015
- [4] Todros T, Sciarrone A, Piccoli E, Guiot C, Kaufmann P, Kingdom J. Umbilical Doppler waveforms and placental villous angiogenesis in pregnancies complicated by fetal growth restriction. *Obstetrics and Gynecology*. 1999;**93**(4):499-503. DOI: 10.1016/S0029-7844(98)00440-2
- [5] Todros T, Piccoli E, Rolfo A, Cardropoli S, Guiot C, Gaglioti P, Oberto M, Vasario E, Canigga I. Review: Feto-placental vascularization: A multifaceted approach. *Placenta*.

2011;**32**(Supplement B, Trophoblast Research Vol. 25):S165-S169. DOI: 10.1016/j.placenta.2010.12.020

- [6] Brunelli R, Masselli G, Parasassi T, De Spirito M, Papi M, Perrone G, Pittaluga E, Gualdi G, Pollettini E, Pittalis A, Anceschi MM. Intervillous circulation in intra-uterine growth restriction. Correlation to fetal well being. *Placenta*. 2010;**31**:1051-1056. DOI: 10.1016/j.placenta.2010.09.004
- [7] Huen I, Morris DM, Wright C, Parker GJM, Sibley CP, Johnstone ED, Naish JH. R1 and R2* changes in the human placenta in response to maternal oxygen challenge. *Magnetic Resonance in Medicine*. 2013;**70**(5):1422-1433. DOI: 10.1002/mrm.24581
- [8] Raine-Fening NJ, Campbell BK, Clewes JS, Kendall NR, Johnson IR. The reliability of virtual organ computer-aided analysis (VOCAL) for the semi quantification of ovarian, endometrial and subendometrial perfusion. *Ultrasound in Obstetrics & Gynecology*. 2003;**22**:633-639. DOI: 10.1002/uog.923
- [9] Morel O, Grangé G, Fresson J, Schaaps JP, Foidart JM, Cabrol D, Tsatsaris V. Vascularization of the placenta and the subplacental myometrium: feasibility and reproducibility of a three-dimensional power Doppler ultrasound quantification technique. A pilot study. *The Journal of Maternal-Fetal & Neonatal Medicine*. 2011;**24**(2):284-290. DOI: 10.3109/14767058.2010.486845
- [10] Kaufmann P, Sen DK, Schweikhart G. Classification of human placental villi: I. Histology. *Cell and Tissue Research*. 1979;**200**:409-423. DOI: 10.1007/BF00234852
- [11] Leiser R, Luckhardt M, Kaufmann P, Winterhager E, Bruns U. The fetal vascularization of term human placental villi. I. Peripheral stem villi. *Anatomy and Embryology (Berlin)*. 1985;**173**(1):71-80. DOI: 10.1007/BF00707305
- [12] Kaufmann P, Bruns U, Leiser R, Luckhardt M, Winterhager E. The fetal vascularisation of term human placental villi. II. Intermediate and terminal villi. *Anatomy and Embryology (Berlin)*. 1985;**173**(2):203-214. DOI: 10.1007/BF00316301
- [13] Happe H. Beobachtungen an eihäuten junger menschlicher eier [Observation at embryonic membranes of early human embryos]. *Anatomische Hefte*. 1906;**32**(2):172-212
- [14] Krantz KE, Parker JC. Contractile properties of the smooth muscle in the human placenta. *Clinical Obstetrics and Gynecology*. 1963;**6**:6-38
- [15] Graf R, Langer JU, Schönfelder G, Öney T, Hartel-Schenk S, Reuter W, Schmidt HHHW. The extravascular contractile system in the human placenta: Morphological and immunocytochemical investigations. *Anatomy and Embryology (Berlin)*. 1994;**190**:541-548. DOI: 10.1007/BF00190104
- [16] Graf R, Schönfelder G, Mühlberger M, Gutsann M. The perivascular contractile sheath of human placental stem villi: Its isolation and characterization. *Placenta*. 1995;**16**:57-66. DOI: 10.1016/0143-4004(95)90081-0

- [17] Graf R, Neudeck H, Gossrau R, Vetter K. Elastic fibres are an essential component of human placental stem villous stroma and an integrated part of the perivascular contractile sheath. *Cell and Tissue Research*. 1996;**283**:131-141. DOI: 10.1007/s004410050521
- [18] Kohnen G, Kertschanska S, Demir R, Kaufmann P. Placental villous stroma as a model system for myofibroblast differentiation. *Histochemistry and Cell Biology*. 1996;**105**:415-429. DOI: 10.1007/BF01457655
- [19] Graf R, Matetjevic D, Schuppan D, Neudeck H, Shakibaei M, Vetter K. Molecular anatomy of the perivascular sheath in human placental stem villi: The contractile apparatus and its association to the extracellular matrix. *Cell and Tissue Research*. 1997;**290**:601-607. DOI: 10.1007/s004410050965
- [20] Demir R, Kosanke G, Kohnen G, Kertschanska S, Kaufmann P. Classification of human placental stem villi: Review of structural and functional aspects. *Microscopy Research and Technique*. 1997;**38**:28-41. DOI: 10.1002/(SICI)1097-0029(19970701/15)38:1/2<29::AID-JEMT5>3.0.CO;2-P
- [21] Farley AE, Graham CH, Smith GN. Contractile properties of human placental anchoring villi. *American Journal of Physiology. Regulatory, Integrative and Comparative Physiology*. 2004;**287**:R680-R684. DOI: 10.1152/ajpregu.00222.2004
- [22] Lecarpentier E, Claes V, Timbely O, Hébert JL, Arsalane A, Moumen A, Guerin C, Guizard M, Michel F, Lecarpentier Y. Role of both actin-myosin cross bridges and NO-cGMP pathway modulators in the contraction and relaxation of human placental stem villi. *Placenta*. 2013;**34**:1163-1169. DOI: 10.1016/j.placenta.2013.10.007
- [23] Lecarpentier Y, Claes V, Lecarpentier E, Guerin C, Hébert JL, Arsalane A, Moumen A, Krokidis X, Michel F, Timbely O. Ultraslow myosin molecular motors of placental contractile stem villi in humans. *PLoS One*. 2014;**9**:e108814. DOI: 10.1371/journal.pone.0108814
- [24] Kato Y, Oyen ML, Burton GJ. Villous tree model with active contractions for estimating blood flow conditions in the human placenta. *The Open Biomedical Engineering Journal*. 2017;**11**:36-48. DOI: 10.2174/1874120701711010036
- [25] Kaufmann P, Luckhardt M, Shweikhart G, Cattle SJ. Cross-sectional features and three-dimensional structure of human placental villi. *Placenta*. 1987;**8**:235-247. DOI: 10.1016/0143-4004(87)90047-6
- [26] Kingdom JCP, Kaufmann P. Oxygen and placental villous development: Origin of fetal hypoxia. *Placenta*. 1997;**18**:613-621. DOI: 10.1016/S0143-4004(97)90000-X
- [27] Kato Y, Oyen ML, Burton GJ. Placental villous tree models for evaluating the mechanical environment in the human placenta. In: *Proceedings of the 2014 IEEE International Conference on Imaging Systems and Techniques (IST)*; 14-17 October 2014; Santrini. IEEE; 2014. pp. 107-111. DOI: 10.1109/IST.2014.6958455

- [28] Todros T, Marzioni D, Lorenzi T, Piccoli E, Capparuccia L, Perugini V, Cardaropoli S, Romagnoli R, Gesuita R, Rolfo A, Paulesu L, Castelluci M. Evidence for a role of TGF- β 1 in the expression and regulation of α -SMA in fetal growth restricted placentae. *Placenta*. 2007;**28**:1123-1132. DOI: 10.1016/j.placenta.2007.06.003
- [29] Pearce P, Brownbill P, Janáček J, Jirkovská M, Kubínová L, Chernyavsky L, Jensen OE. Image-based modeling of blood flow and oxygen transfer in fetoplacental capillaries. *PLoS One*. 2016;**11**(10):e165369. DOI: 10.1371/journal.pone.0165369
- [30] Suci L, Popescu LM, Gherghiceanu M. Human placenta: *de visu* demonstration of interstitial Cajal-like cells. *Journal of Cellular and Molecular Medicine*. 2007;**11**(3):590-597. DOI: 10.1111/j.1582-4934.2007.00058.x
- [31] Popescu LM, Faussone-Pellegrini MSF. Telocytes—A case of serendipity: The winding way from interstitial cells of Cajal (ICC) *via* interstitial Cajal-like cells (ICLC) to telocytes. *Journal of Cellular and Molecular Medicine*. 2010;**14**(4):729-740. DOI: 10.1111/j.1582-4934.2010.01059.x
- [32] Bosco C, Díaz. Presence of telocytes in a non-innervated organ: The placenta. In: Wang X, Cretoiu E, editors. *Telocytes—Connecting Cells (Advances in Experimental Medicine and Biology)*. Singapore: Springer Science+Business Media Singapore; 2016. pp. 149-161. DOI: 10.1007/978-981-10-1061-3
- [33] Nizyaeva NV, Sukhacheva TV, Serov RA, Kulikova GV, Nagovitsyna MN, Kan NE, Tyutyunnik VL, Pavlovich SV, Poltavtseva RA, Yarotskaya EL, Shchegolev AI, Sukhikh GT. Ultrastructural and immunohistochemical features of telocytes in placental villi in preeclampsia. *Scientific Reports*. 2018;**8**:3453. DOI: 10.1038/s41598-018-21492-w
- [34] Hasegawa J, Suzuki N. SMI for imaging of placental infarction. *Placenta*. 2016;**47**:96-98. DOI: 10.1016/j.placenta.2016.08.092

